Correlation between Optical Properties and Chain-Length in a Quasi-One-Dimensional Electronic Polymer

Jui-Hung Hsu,[†] Michi-toshi Hayashi,[‡] Sheng-Hsien Lin,[†] Wunshain Fann,*[,†,§] Lewis J. Rothberg,[||] Gung-Yeong Perng,[⊥] and Shaw-An Chen[⊥]

Institute of Atomic and Molecular Sciences, Academia Sinica, P.O. Box 23-166, Taipei, Taiwan, ROC, Center for Condensed Matter Sciences, National Taiwan University, Taipei, Taiwan, Department of Physics, National Taiwan University, Taipei, Taiwan, Department of Chemistry, University of Rochester, Rochester, New York 14627, and Department of Chemical Engineering, National Tsing-Hwa University, Hsinchu, Taiwan

Received: January 25, 2002; In Final Form: June 14, 2002

We study the molecular weight dependence of the photophysics of a soluble electroluminescent conjugated polymer DOO-PPV in dilute chloroform solution. The absorption and the fluorescence maxima red-shift progressively with increasing weight as the average chain length increases from approximately 9 to 30 monomer units. At the same time, the fluorescence yield of the polymer decreases even though the radiative rate is found to increase. This behavior is caused by a rapid increase in nonradiative decay as the optical gap of the polymer decreases, and we present a quantitative theory that satisfactorily accounts for the dominance of multiphonon relaxation via internal conversion. We also find that the polymer length at which the optical properties saturate is considerably longer than predicted by theoretical calculations of electronic coherence length or by modeling of absorption data using the Strickler-Berg relationship.

1. Introduction

Conjugated systems are endowed with electrical and optical properties that permit various interesting applications.[1,2] In a quasi-one-dimensional conjugated polymer, the delocalization of π electrons along its backbone reduces the HOMO-LUMO gap to that of a typical semiconductor. One of the critical scientific and technological issues in conjugated polymer research is a question as to how the chain-length affects the electronic properties. One example of interest is the chain-length dependence of the absorption spectrum and third-order nonlinear susceptibilities of well-defined linear polyene oligomers as reported by Samuel et al.[3−6] They observed the surprising result that the third-order nonlinearity per unit double bond, γ/N, does not saturate as far as a length up to 60 double bonds. To explain the anomalously long saturation lengths, Kohler et al. invoked a model in which defects lead to a distribution of short conjugation segments in the long chain polymer.[6,7] Recent studies of oligomers of the technologically important conjugated polymer, poly(*p*-phenylene vinylene) (PPV), suggest that the effective chain length in PPV, based on a linear relation between the energy gap and the reciprocal number of monomer units, m^{-1}, is between 7 and 10 monomers.[8,9] However, investigation of longer chain oligomers in solution reveals a deviation from that reciprocal relation that implies a much higher saturation chain length in the polymer solution. Theoretical calculations also support the high saturation chain length behavior.[10] The situation is complicated by the fact that heptamers and octomers exhibit identical photoluminescence in the solid state, while in solution cyclic voltammetry indicates a distinctly reduced energy gap for the octomer.[11] Different saturation lengths in solution and film are rationalized by reflecting strong intermolecular interaction in the films.[12] It should be noted that saturation of different optical properties can be due to different mechanisms. For example, the saturation of band-gap absorption could be dictated by delocalization of the band-gap exciton, whereas the saturation of the third-order nonlinear response could be governed by delocalization of several electronic states contributing into these spectra. On the other hand, the red-shift of the photoluminescence with the chain size could be explained by exciton migration to longer conjugated segments.

In this paper, the photophysical properties of different molecular weight samples of poly(2,5 dioctyloxy *p*-phenylenevinylene), DOO-PPV, in dilute solution are addressed. We study the saturation of the linear optical properties, absorption spectra, emission spectra, and exciton lifetime versus chain length and compare these with predictions of the theory for quasi-one-dimensional extended electronic semiconductors. The synthesis of moderate molecular weight soluble conjugated polymers typically results in a broad distribution of chain lengths and we isolate relatively narrow distributions using molecular weight-dependent solubility.[13−15]

2. Experimental Methods

The synthetic procedure and the optical properties of DOO-PPV are described elsewhere.[16] The molecular weight of the pristine polymer is estimated to be 2 million Dalton by gel permeation chromatography (GPC) calibrated with polystyrene standards. Due to the symmetrically substituted structure, DOO-PPV can only be well dissolved in a limited number of solvents. Polydispersed samples can therefore be sorted out using different solvents. Those having large mismatch in solubility parameter with the phenylenevinylene moiety will only dissolve low molecular weight segments so that sequential exposure to a series of solvents with smaller mismatch results in separation

* Corresponding author.
[†] Institute of Atomic and Molecular Sciences, Academia Sinica.
[‡] Center for Condensed Matter Sciences, National Taiwan University.
[§] Department of Physics, National Taiwan University.
[||] Department of Chemistry, University of Rochester.
[⊥] Department of Chemical Engineering, National Tsing-Hwa University.

10.1021/jp025556i CCC: $22.00
Published on Web 08/02/2002

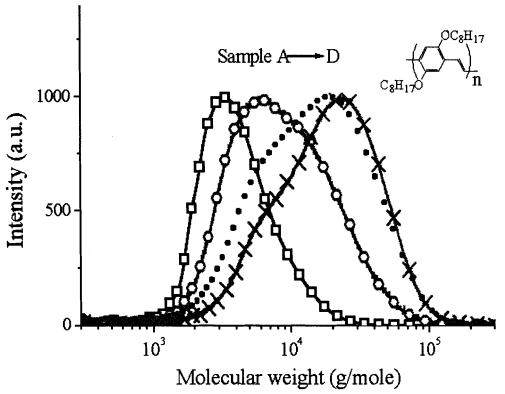

Figure 1. GPC results for samples A to D. The average molecular weights of A to D are 3.2K, 5.6K, 8.2K, and 11K, respectively. Sample E has a molecular weight of $\sim 2M$, much larger than that of D. The chemical structure of DOO-PPV is shown in inset.

of the polydispersed sample into relatively narrow molecular weight distributions.[17] In addition, we can adjust the solubility in a given solvent with temperature. Lower temperatures lead to preferential solubility for short segments due to entropic considerations.

Our fractionation procedure is as follows. The solid polydispersed DOO-PPV is immersed in toluene at 0 °C. After a few hours, the undissolved polymer powder is separated from the solution. Sample A is obtained by drying the filtered solution under nitrogen. The residual polymer powder is rinsed by cold toluene and cold chloroform and immersed in 0 °C chloroform. After a few hours, the undissolved powder is again separated and sample B results after drying the filtered solution under nitrogen. The residual polymer is dissolved into chloroform solution at 24 °C and then dried to obtain sample C. In the final step, the remaining undissolved polymer is dissolved in chloroform solution at 40 °C and dried to produce sample D. The remaining powder is dried to yield sample E.

The molecular weights of samples A through D are estimated by gel permeation chromatography (GPC) using tetrahydrofuran as the solvent, as shown in Figure 1. The GPC column temperature is raised to 45 °C to increase the solubility. Molecular weights are calibrated by polystyrene standards under the same conditions. The number-average molecular weights of A to D are 3.2K, 5.6K, 8.2K, and 11K, with polydispersity (δ), M_w/M_n, of 1.38, 1.87, 2.23, and 1.98, respectively. These correspond to average lengths of 9, 16, 23, and 31 monomer units. Note that M_w measured here is not the absolute molecular weight, but the molecular weight calibrated with respect to polystyrene standard.[4,5] Because even the polystyrene standard exhibits finite-width in our GPC results, the actual polydispersity of the samples should be significantly narrower than the measured values. It is important to bear in mind that most of the pristine polymer remains in the powder even after our final fractionation step. Thus, the molecular weight of sample E is much higher than that of sample D, roughly that pristine polymer ($\sim 2M$).

3. Results and Discussions

For spectroscopic studies, samples A to E are dissolved into dilute chloroform solution (approximately 10^{-6} M in monomer unit). Chloroform is an excellent solvent for the polymer where aggregation effects can be considered negligible. Figure 2 demonstrates that the absorption maximum shifts progressively to longer wavelength as the chain length increases from A to D. Normalizing the absorption maximum of the lowest electronic band as done in the figure illustrates that the relative oscillator

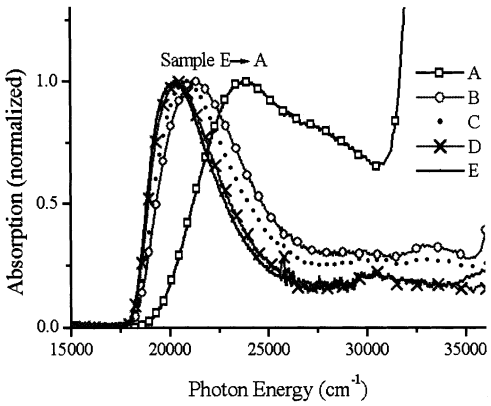

Figure 2. Absorption spectra of DOO-PPV in dilute chloroform solution from A (open square) to E (solid line).

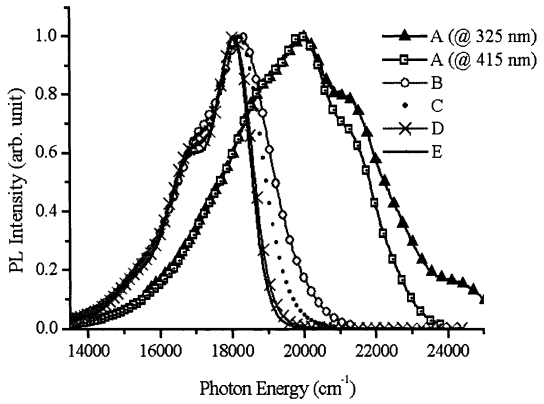

Figure 3. Fluorescence spectra of A to E in dilute chloroform solution. The spectra of sample A are excited at 325 and 415 nm, respectively.

strength carried by the lowest band increases with chain length as expected theoretically.

Figure 3 presents the fluorescence spectra of samples A to E. Sample A has an excitation wavelength-dependent PL spectrum reflecting the rapid change of properties that occurs with chain length for short chains. This inhomogeneity also explains the unusually broad absorption spectra of sample A. As in absorption, the fluorescence spectra of samples A to D progressively exhibit red shifts.

The electronic energy gap and Huang-Rhys factor are estimated by the following equations. The absorption and fluorescence spectra for the optical transition between the electronic ground state $|a\rangle$ and excited state $|b\rangle$ can be given by

$$\alpha_{a\to b}(\omega) \propto e^{-S}\sum_n \frac{S^n}{n!} D(\omega - \omega_{ba} - n\omega_p) \tag{1a}$$

$$I_{b\to a}(\omega) \propto e^{-S}\sum_n \frac{S^n}{n!} D(\omega_{ba} - n\omega_p - \omega) \tag{1b}$$

$$D(\omega - \omega_{ba} - n\omega_p) = \int_{-\infty}^{\infty} dt \exp[it(\omega - \omega_{ba} - n\omega_p) - |t|\gamma_{ba}] \tag{1c}$$

where ω_{ab} is the electronic energy gap, ω_p is the phonon mode frequency, and S is the Huang-Rhys factor:

$$S = {}^1/_2(M\omega_p/\hbar)(\Delta Q)^2 \tag{1d}$$

where M is the reduced mass of the vibrational mode and ΔQ is the change of equilibrium displacement of the ground and

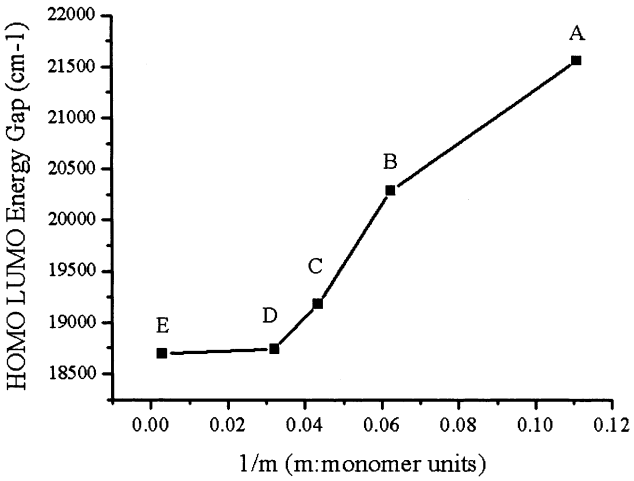

Figure 4. The HOMO-LUMO energy gap versus the inverse number of monomer units for samples A to E

excited states. Here γ_{ba} in eq 1c denotes the dephasing rate constant and in the numerical calculation, this constant is used as a convergent factor.

By fitting the observed absorption and fluorescence spectra, respectively, to eqs 1a and 1b simultaneously, we can determine ω_{ba}, ω_p and S. We thus obtain the electronic energy gap for each system as (A) 21561 cm^{-1}, (B) 20290 cm^{-1}, (C) 19180 cm^{-1}, (D) 18740 cm^{-1}, and (E) 18690 cm^{-1}. Figure 4 plots the electronic energy gap position versus m^{-1} (inverse monomer units) and shows saturation behavior. Samples D and E exhibit nearly the same spectra even though the average chain length of sample E is much larger than that of D. Thus, the length of D (about 30 monomers) is about the saturation length in our samples and is much longer than the conjugation length for the same reasons discussed by Kohler.

The Huang-Rhys factors for different chain length samples are obtained as (A) 1.55, (B) 0.606, (C) 0.605, (D) 0.575, and (E) 0.566. The Huang-Rhys factors can also be estimated roughly from the ratio of secondary vibronic peak (1−0 transition) to the first peak (0−0 transition) in the fluorescence spectrum. The results shows that S decreases as the chain-length increases. This trend reflects weaker electron−phonon coupling in the longer chain polymers and is consistent with theoretical calculations and previous experimental work.[18−20] The purified polymer E has a quite narrow fluorescent spectrum since it consists of all chains with at least thirty units whose properties are uniformly in the long chain limit. In fact, a comparison between the absorption and fluorescence excitation spectra of sample E shows that they are identical, as shown in Figure 5. This means that the PL yield is excitation wavelength independent (Kasha's Rule) as is characteristic of homogeneous systems. The small number of short chains in the unfractionated ("pristine") samples produce a slightly higher blue/UV absorption that does not lead to emission at the wavelength being monitored so that a deviation of the absorption from the PL excitation spectrum (identical to that of E) is observed. We point this out to illustrate that wavelength-dependent quantum yield may only reflect chain length inhomogeneity but not fundamental changes in photophysics as have sometimes been invoked to explain it.

Other effects of chain length distribution occur in the PL spectrum and the corresponding decay dynamics. For example, sample E is missing the blue emission observed in the pristine sample (Figure 6a) that comes from the short chain polymers. With the excited-state lifetime depending on conjugation length,

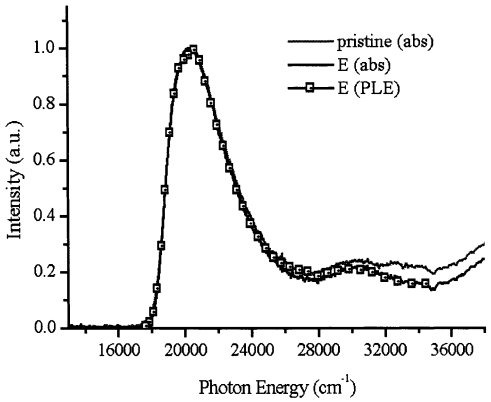

Figure 5. The absorption spectra of the pristine polymer, sample E, and the fluorescence excitation spectrum of sample E. Absorption spectra are plotted on a linear scale to directly compare with excitation spectra.

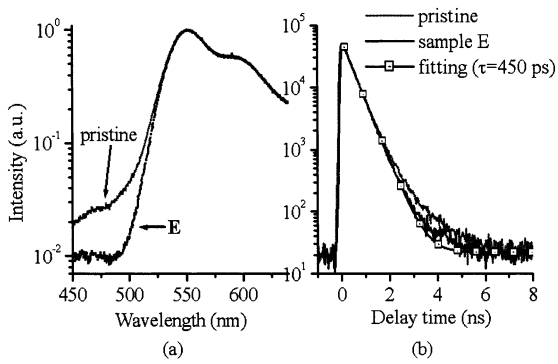

Figure 6. (a) Both the PL spectra of the pristine polymer (gray line) and sample E (dark line) excited at 400 nm; the vertical scale is plotted on a log scale. (b) The PL decay of sample E and the pristine polymer; the single-exponential fit of sample E corresponds to a decay time of 450 ps.

spectral dynamics in the fluorescence decay can also result from sample inhomogeneity. In the long chain sample E, the PL decay is single exponential and wavelength independent (Figure 6b). The PL dynamics of samples A through C, however, exhibit multiexponential relaxation due to the contributions of several distinct conjugation lengths and, consequently, the decay dynamics also depends on the monitored wavelength. The fluorescence dynamics of the pristine sample, illustrated in Figure 6b, also show a deviation from single-exponential behavior since short chains contribute. In summary, the photophysical properties of our pristine samples can be explained by chain length inhomogeneity.

The dependence of oligomer length on the excited-state decay rate was reported previously.[21,22] This behavior is also observed in our different length polymer samples. Althought multiexponential fits are used to derive mean decay rates versus molecular weight for samples A to D, dominated term exists in decay dynamics. For example, at the emission maximum, the fluorescent intensity contribution from dominated decay component is 75 and 95% for sample B and C, respectively. Even in samples C and D where the PL spectra are similar large differences in excited-state lifetimes are observed ($\tau_C \approx 580$ ps $> \tau_D \approx 490$ ps). The radiative and nonradiative decay rates, k_r and k_{nr}, are related to both quantum yields and fluorescence decay rates, that is,[23,24]

$$\text{fluorescence decay rate} = k_r + k_{nr} \tag{2a}$$

$$\text{quantum yields} = \Phi^*\{k_r/(k_r + k_{nr})\} \tag{2b}$$

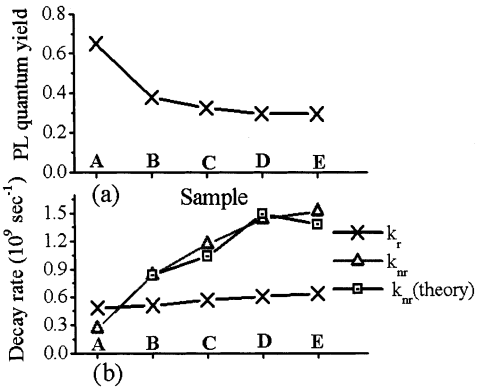

Figure 7. (a) Fluorescence quantum yields and (b) radiative (dark cross), k_r, nonradiative (gray triangle), k_{nr}, decay rates of species A to E. The calculated nonradiative decay rates (dark square) based on a single phonon mode model are shown for comparison.

where Φ^* is the photogenerating efficiency of the singlet intrachain excitons. For PPV-type polymer in solution, it is generally accepted that $\Phi^* = 1$. Thus combining the measured quantum yields and fluorescence decay rates allows us to extract average radiative and nonradiative rates. Results are summarized along with the quantum yields in Figure 7. As the chain length increases, the PL quantum yield *decreases* from 0.65 (A) to 0.3 (E), shown in Figure 7a. At the same time, the corresponding radiative decay rates *increase* from 0.48×10^9 s^{-1}(A) to 0.64×10^9 s^{-1}(E), shown in Figure 7b. We are forced to rationalize this behavior by postulating that the nonradiative rate increases even more rapidly with molecular weight.

The radiative decay rate data can be used to test the applicability of the Strickler-Berg (modified Einstein) relationship between radiative rates k_r and the experimentally measured integrated extinction coefficient in the absorption spectrum[25]

$$k_r = \left[2.88 \times 10^{-9} n^2 \frac{g_a}{g_b} \int \frac{\epsilon(\bar{\nu})}{\bar{\nu}} d\bar{\nu}\right] \frac{\int I(\bar{\nu})\, d\bar{\nu}}{\int \bar{\nu}^{-3} I(\bar{\nu})\, d\bar{\nu}} \qquad (3)$$

where g_a and g_b are the degenerates of the lower and upper states, $\bar{\nu}$ is the refractive index, ϵ is the molar absorption coefficient, I is the normalized emission intensity, and $\bar{\nu}$ is the wavenumber $2\pi/\lambda$. A prescription for how to count the number of chromophores in a system where the number of unit cells is much larger than the electronic coherence length is essential. We assume here that the long polymer chain is comprised of several independent chromophore segments of about one conjugation length and that each segment contributes its corresponding transition strength. The extinction coefficient of the long chain DOO-PPV at the absorption peak is measured to be 1.6×10^4 M^{-1} cm^{-1} per monomer unit. Use of the Strickler-Berg relationship then yields an effective chromophore size of approximately seven monomer units for the experimentally observed radiative decay rate. As is clear from our data, this value is less than half of the experimental result for saturation chain length at room temperature, indicating that the Strickler-Berg relationship cannot be used quantitatively. The anomalously long saturation length is reminiscent of the work of Samuel and Kohler on nonlinear optical properties of polyenes cited in the Introduction. We tentatively ascribe a similar explanation to our data, namely that random conjugation defects lead to an overestimate of the coherence length.

Figure 7 also shows that the nonradiative decay rates increase more rapidly with chain length than do the radiative rates. To show that this is plausible, we have developed a theory to estimate nonradiative decay rate constants k_{nr} (i.e., rates for internal conversion) using a single vibrational mode multiquantum relaxation model. In the model, the vibrational mode acts as both a promoting mode for the nonradiative transition and as the optically active mode in the fluorescence and absorption spectra. From the structure in the optical spectra we adopt the 1430 cm^{-1} backbone stretch as the single mode for sample B to E. The nonradiative rate constant for internal conversion from the excited state $|b\rangle$ to the ground state $|a\rangle$ can then be approximated, using the saddle point method, by[26,27]

$$k_{b\to a} \propto \sqrt{\frac{2\pi}{\omega_p(\omega_{ba} - \omega_p)}} \exp\left[-S - \frac{(\omega_{ba} - \omega_p)}{\omega_p}\left\{\ln\left(\frac{\omega_{ba} - \omega_p}{S\omega_p}\right) - 1\right\}\right] \qquad (4)$$

Figure 7b shows the results from eq 4 for our simplified model of DOO-PPV and all spectra are normalized with respect to sample B. One can see that the calculated nonradiative rate constant $k_{b\to a}$ increases with an increase in molecular weight. This tendency is in good agreement with experiment. Equation 4 shows that there are two contributions to the nonradiative rate constant: (i) the exponential pre-factor that is a function of the energy gap, and (ii) the exponential factor that is a function of the energy gap and Huang-Rhys factor. Our theoretical fitting based on eq 4 shows that all values of the Huang-Rhys factor are less than 1 and a change from the samples C to D is within 5% and 1.5% from D to E. In this case, the energy gap is a dominant factor in the exponential factor in eq 4. On the other hand, the exponential pre-factor only varies within 1.3% to 2.6%. Therefore, the energy gap in the exponential function is the dominant factor to the nonradiative rate constant in the short chain polymers. Note that this tendency is not sensitive to changes ($\pm$10%) in the values used in this calculation.

Sample A does not agree well with experiment, probably because it consists of a relatively wide range of subsystems. This system contains various greatly different optical species and we cannot correctly characterize this system by using the single mode model. Note that the molecular weight of E and D is different by 2 orders of magnitude; sample D has a chain length close to the persistence length, hence more like a rodlike structure, while sample E folds into coil-like structures.[28] However, they both follow the same rule for nonradiative relaxation. It should also be noted that we have obtained good agreement while assuming the nonradiative relaxation rate is intrinsic and not due to defects in the materials or end effects of some kind.

The polymer length that the optical properties saturated reported in this paper is longer than that reported by Meier et al. in oligomer studies.[29] We find the previous results to be surprising. While oligomers are nominally monodispersed, they still have an effective distribution of conjugation lengths introduced by dynamic torsional disorder of the phenyl rings. Tretiak and co-workers have showed that torsional disorder is important to the band shapes and absorption edges of phenylenevinylene oligomers and can also explain the evolution of Franck-Condon envelope with chain length.[30] From a spectroscopic point of view, these dynamic twisting "defects" act much like static conjugation defects in that they restrict the electronic delocalization length. One therefore expects to observe the lowest possible optical gap only when the torsional order extends farther than the spread of the excitonic wave function on an ideal frozen chain. It is much more probable to find segments of a chain that are close to that geometry when the chain is

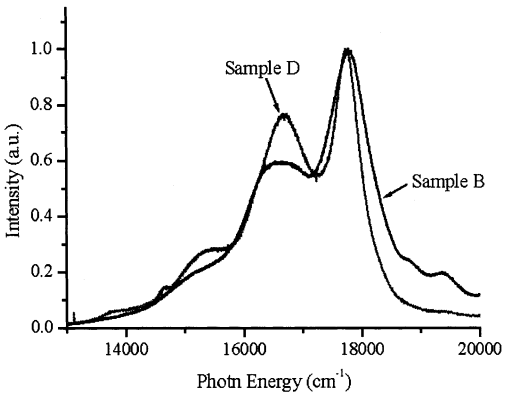

Figure 8. PL spectra of sample B and D in 2-methyltetrahyrofuran solutions measured at 77 K.

much longer and the emission therefore continues to red-shift even as the chain is increased beyond the maximum exciton size. We would predict on the basis of this picture that convergence of the optical gap would occur at much shorter chain lengths at very low temperatures where torsion is frozen out. Figure 8 shows the low-temperature single chain emission spectra of samples B and D in 2-methyltetrahydrofuran dilute solution at 77 K. At liquid nitrogen temperature, *m*-THF solution forms a dilutely doped glass where aggregation is negligible. Although samples B and D have different PL spectra at room temperature, sample B exhibits an almost identical PL peak position to that of D (difference only by 1 nm), at low temperature. These results are consistent with our explanation above that the anomalously long saturation length in the 300 K data being a result of torsional disorder.

4. Conclusion

A chain separation method based on chain length-dependent solubility is developed. Polymer samples in solution that are purified to eliminate short chains follow classical molecular photophysical behavior including single exponential excited-state decay dynamics and excitation wavelength-independent luminescence quantum yield. As molecular weight increases, we observe collapse of oscillator strength into the lowest optical transition as expected by the theory for low-dimensional semiconductors. This concentration of transition strength in the lowest band results in an increased radiative decay rate for longer polymer chains. Even so, smaller quantum yield for luminescence is observed due to rapidly increasing nonradiative relaxation as the HOMO-LUMO gap decreases. We show that this is a consequence of the dependence of internal conversion rate on the HOMO-LUMO gap. The variation of optical properties such as the HOMO-LUMO gap with chain length continues even beyond what we believe to be the intrinsic conjugation length by at least a factor of 2. We ascribe this to a random distribution of defects that determines the actual distribution of uninterrupted conjugation segments on high molecular weight chains and, hence, speculate that it will be sample dependent.[31]

Acknowledgment. We thank H. L. Cheng for assisting with the GPC measurements. This research was supported by the Excellent Project, Education Ministry, Taiwan, ROC and U.S. Army Research Grant DAAD1999-1-0206.

References and Notes

(1) Burroughes, J. H.; Bradley, D. D. C.; Brown, A. R.; Marks, R. N.; Mackay, K.; Friend, R. H.; Burns, P. L.; Holmes, A. B. *Nature* **1990**, *347*, 539.

(2) Friend, R. H.; Gymer, R. W.; Holmes, A. B.; Burroughes, J. H.; Marks, R. N.; Taliani, C.; Bradley, D. D. C.; Dos Santos, D. A.; Bredas, J. L.; Logdlund M.; Salaneck, W. R. *Nature* **1999**, *397*, 121.

(3) Samuel, I. D. W.; Ledoux, I.; Dhenaut, C.; Zyss, J.; Fox, H. H.; Schrock, R. R.; Silbey, R. J. *Science* **1994**, *265*, 1070.

(4) Fox, H. H.; Wolf, M. O.; O'Dell, R.; Lin, B. L.; Schrock R. R.; Wrighton, R. S. *J. Am. Chem. Soc.* **1994**, *116*, 2827.

(5) Ledoux, I.; Samuel, I. D. W.; Zyss, J.; Yaliraki, S. N.; Schattemann, F. J.; Schrock, R. R.; Silbey, R. J. *Chem. Phys.* **1999**, *245*, 1.

(6) Kohler, B. E.; Samuel, I. D. W. *J. Chem. Phys.* **1995**, *103*, 6248.

(7) Kohler, B. E.; Woehl, J. C. *J. Chem. Phys.* **1995**, *103*, 6253.

(8) Tian, B.; Zerbi, G.; Schenk, R.; Müllen, K. *J. Chem. Phys.* **1991**, *95*, 3191.

(9) Graham, S. C.; Bradley, D. D. C.; Friend, R. H.; Spangler, C. *Synth. Met.* **1991**, *41*, 1277.

(10) Oelkrug, D.; Tompert, A.; Egelhaaf, H.-J.; Hanack, M.; Steinhuber, E.; Hohloch, M.; Meier, H.; Stalmach, U. *Synth. Met.* **1996**, *83*, 231.

(11) Gebhardt, V.; Bacher, A.; Thelakkat, M.; Stalmach, U.; Meier, H.; Schmidt, H. W.; Haarer, D. *Adv. Mater.* **1999**, *11*, 119.

(12) Cornil, J.; Heeger, A. J.; Brédas, J. L. *Chem. Phys. Lett.* **1997**, *272*, 463.

(13) Hsieh, B. R.; Anita, Y. Y.; Vanleaken C.; Lee, H. *Macromolecules* **1997**, *30*, 8094.

(14) Sun, S. F. *Physical Chemistry of Macromolecules*; Wiley: New York, 1994.

(15) Barrales-Rienda, J. M.; Bello, A.; Bello, P.; Guzman, G. M. In *Polymer Handbook*, 4th ed.; Brandrup, J., Immergut, E. H., Grulke, E. A., Eds; Wiley-Interscience: New York, 1999; pp VII 32−VII 330.

(16) Hsu, J. H.; Fann, W. S.; Tsao, P. S.; Chuang, K. R.; Chen, S. A. *J. Phys. Chem. A* **1999**, *103*, 2375.

(17) Grulke, E. A. In *Polymer Handbook*, 4th ed.; Brandrup, J., Immergut, E. H., Grulke, E. A., Eds; Wiley-Interscience: New York, 1999; pp VII 675−VII 711.

(18) Chang, R.; Hsu, J. H.; Fann, W. S.; Liang, K. K.; Chang, C. H.; Hayashi, M.; Yu, J.; Lin, S. H.; Chang, E. C.; Chuang, K. R.; Chen, S. A. *Chem. Phys. Lett.* **2000**, *317*, 142.

(19) Cornil, J.; Beljonne, D.; Shuai, Z.; Hagler, T. W.; Campbell, I.; Bradely, D. D. C.; Brédas, J. L.; Spangler, C. W.; Müllen, K. *Chem. Phys. Lett.* **1995**, *247*, 425.

(20) Cornil, J.; Beljonne, D.; Heller, C. M.; Campbell, I. H.; Laurich, B. K.; Smith, D. L.; Bradely, D. D. C.; Müllen K.; Brédas, J. L. *Chem. Phys. Lett.* **1997**, *278*, 139.

(21) Oelkrug, D.; Tompert, A.; Gierschner, J.; Egelhaaf, H.-J.; Hanack, M.; Hohloch, M.; Steinhuber, E. *J. Phys. Chem. B* **1998**, *102*, 1902.

(22) Peeters, E.; Ramos, A. M.; Meskers S. C. J.; Janssen, R. A. J. *J. Chem. Phys.* **2000**, *112*, 9445.

(23) Samuel, I. D. W.; Rumbles, G.; Friend, R. H., In *Primary Photoexcitations in Conjugated Polymers: Molecular Exciton versus Semiconductor Band Model*; Sariciftci, N. S., Eds; World Scientific: Singapore, 1997; pp 140−144.

(24) Turro, N. J. In *Modern Molecular Photochemistry*; University Science Books: Mill Valley, CA, 1991; p 109.

(25) Strickler, S. J.; Berg, R. A. *J. Chem. Phys.* **1962**, *37*, 814.

(26) Lin, S. H. *J. Chem. Phys.* **1966**, *44*, 3759.

(27) Hayashi, M.; Yang, T.-S.; Yu, J.; Mebel, A.; Lin, S. H. *J. Phys. Chem.* **1997**, *101*, 4156.

(28) Gettinger, G. C.; Heeger, A. J.; Drake J. M.; Pine, D. J. *J. Chem. Phys.* **1994**, *101*, 1673.

(29) Meier, H.; Stalmach U.; Kolshorn, H. *Acta Polym.* **1997**, *48*, 379.

(30) Tretiak, S.; Saxena, A.; Martin, R. L.; Bishop, A. R. *Chem. Phys. Lett.* **2000**, *331*, 561.

(31) Grimme, J.; Kreyenschmidt, M.; Uckert, F.; Müllen K.; Scherf, U. *Adv. Mater.* **1995**, *7*, 292.